Energieverlust durch Ionisation:

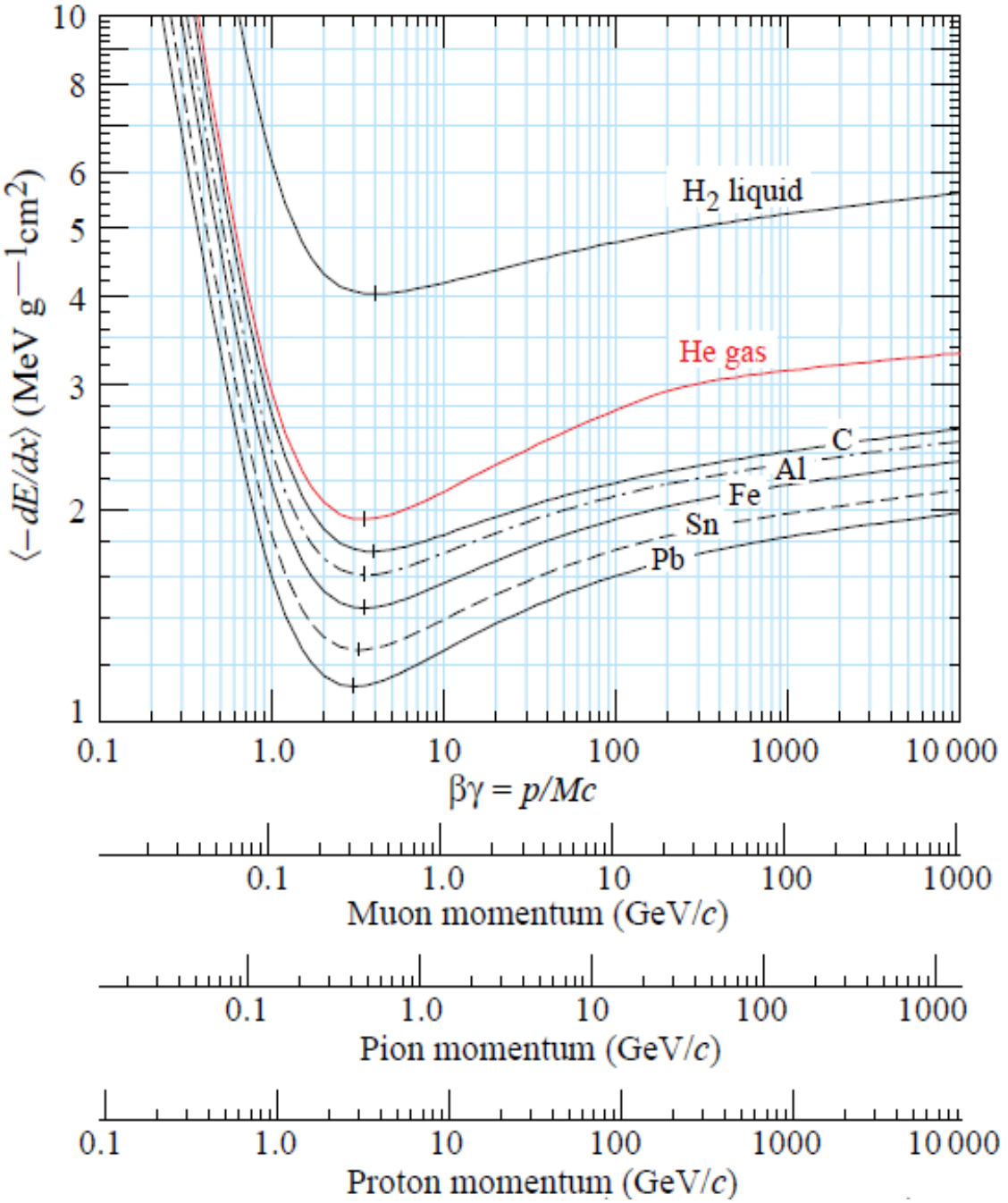

Fig. 3.1

hadronischer Schauer:

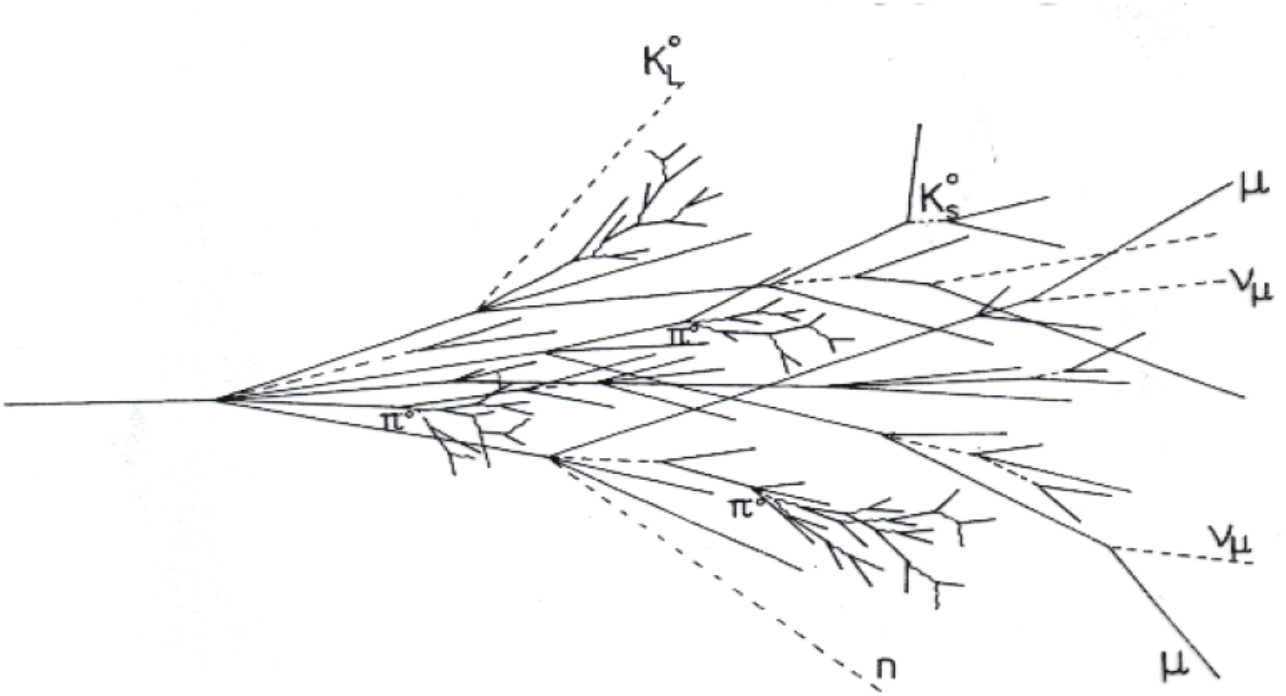

elektromagnetischer Schauer:

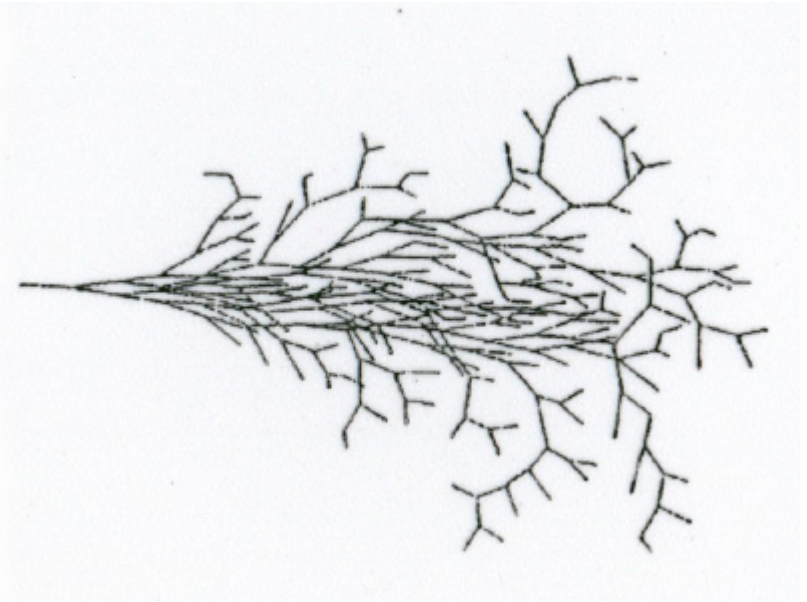

Fig. 3.2

Wechselwirkung von Photonen:

$$\sigma_{tot} = \sigma_{Ph} + \sigma_c + \sigma_p$$

$$\mu = \mu_{Ph} + \mu_c + \mu_p$$

$$\mu_i = n\sigma_i = \frac{N_A \rho}{A}\sigma_i$$

kohärente Streuung am ganzen Atom, weder Ionisation noch Anregung, nicht wichtig als Energieverlustmechanismus

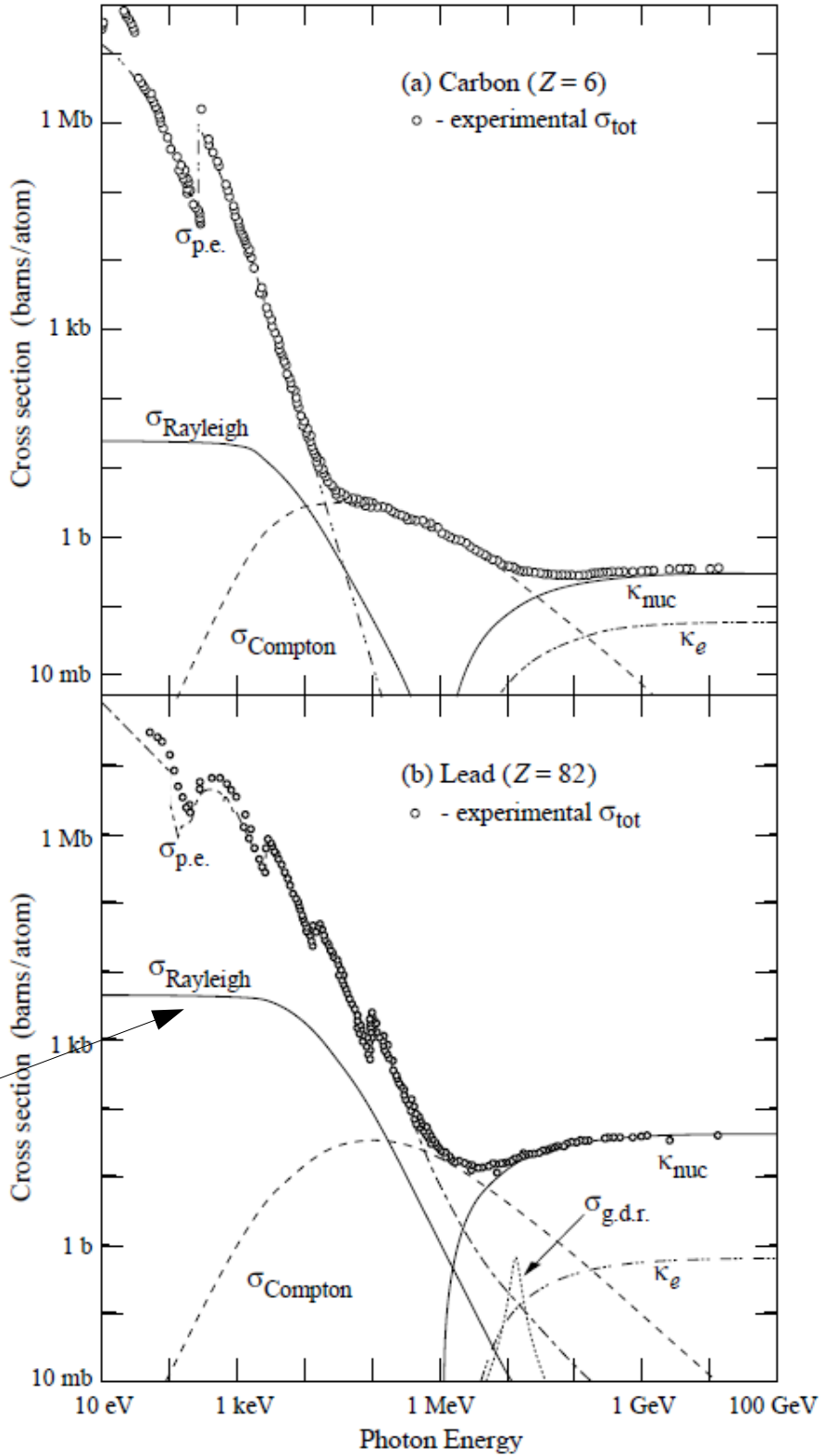

Fig. 3.3

Vorwärtsspektrometer

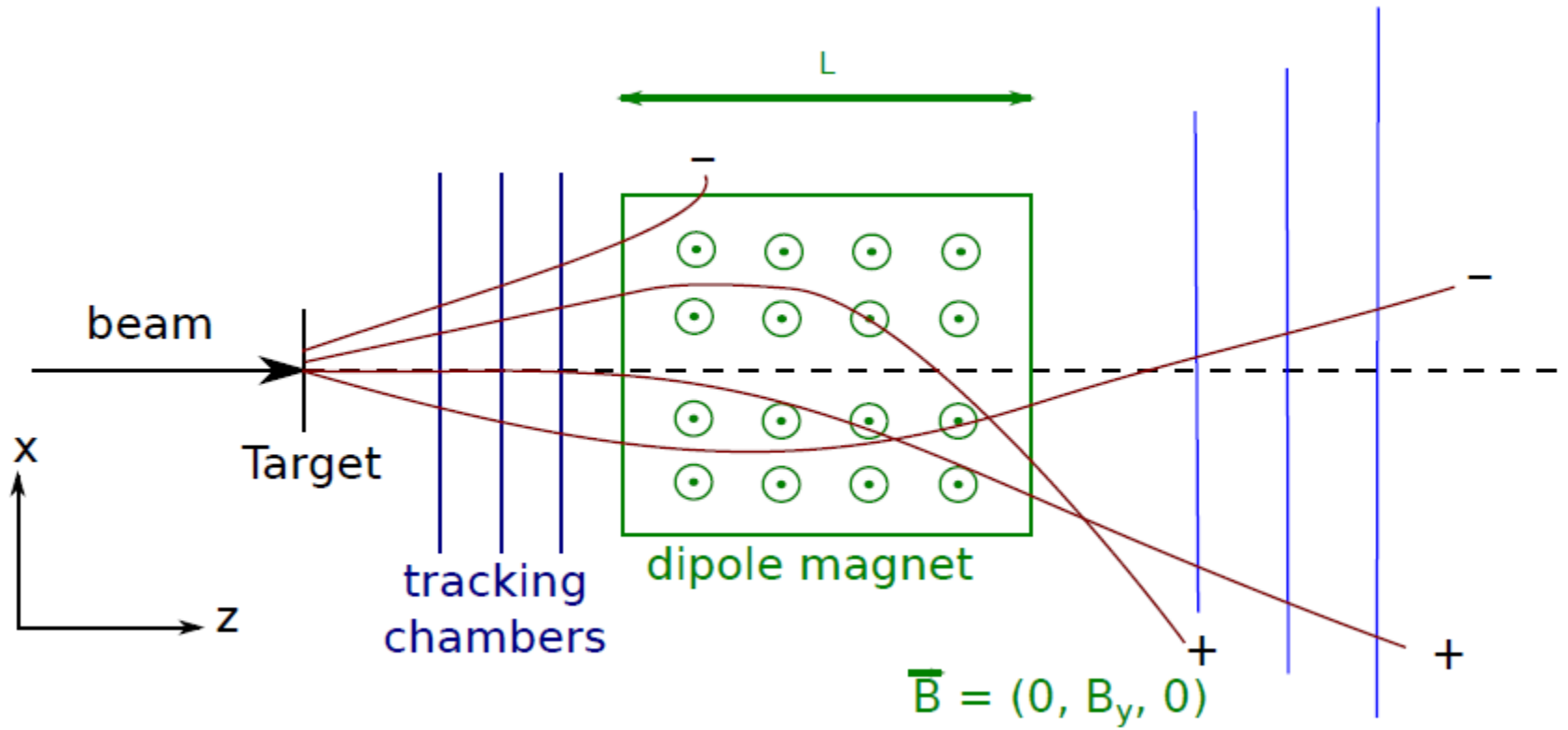

Ablenkung in x,z-Ebene: Messung von mindestens 2 Punkten or dem B-Feld und 2 danach

Fig. 4.1

solenoidales B-Feld

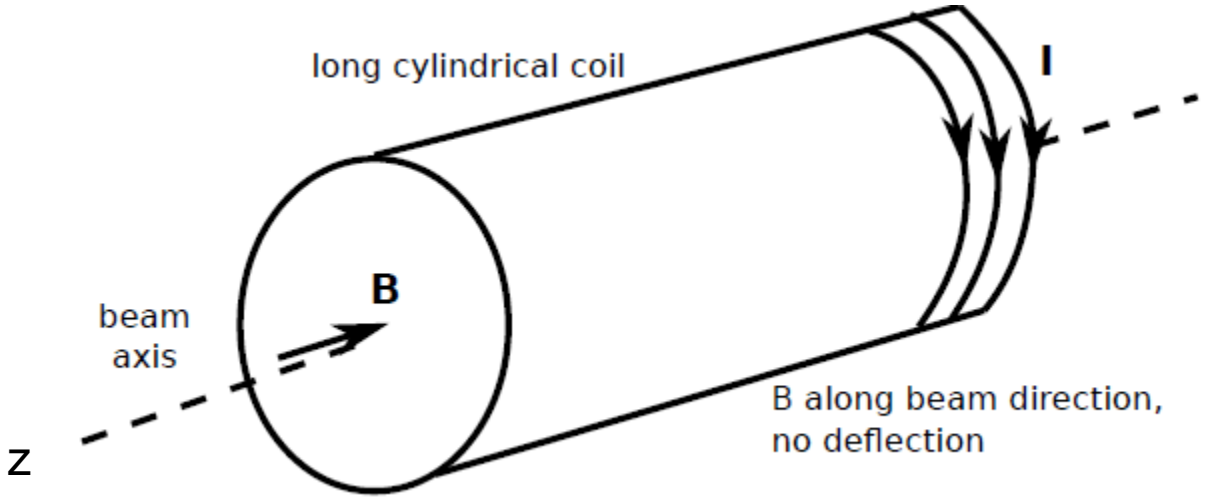

Messung von mindestens 3 Punkten definiert $p_\perp$

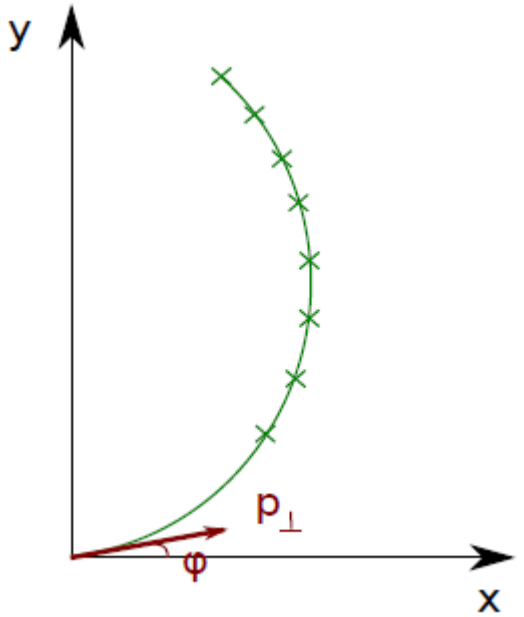

Fig. 4.2

Vieldrahtproportionalkammer

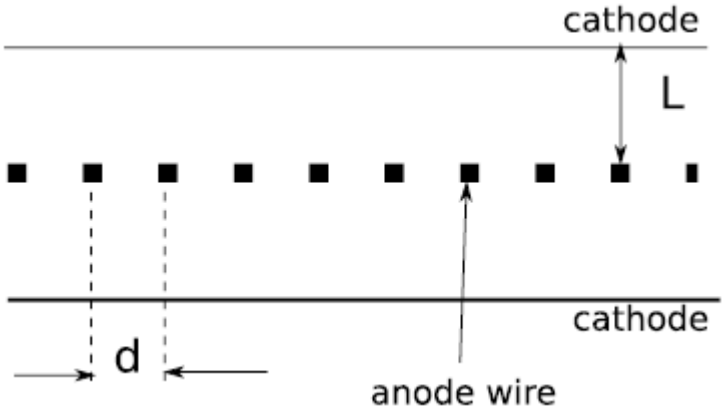

typische Gasverstärkung: 2000-10000

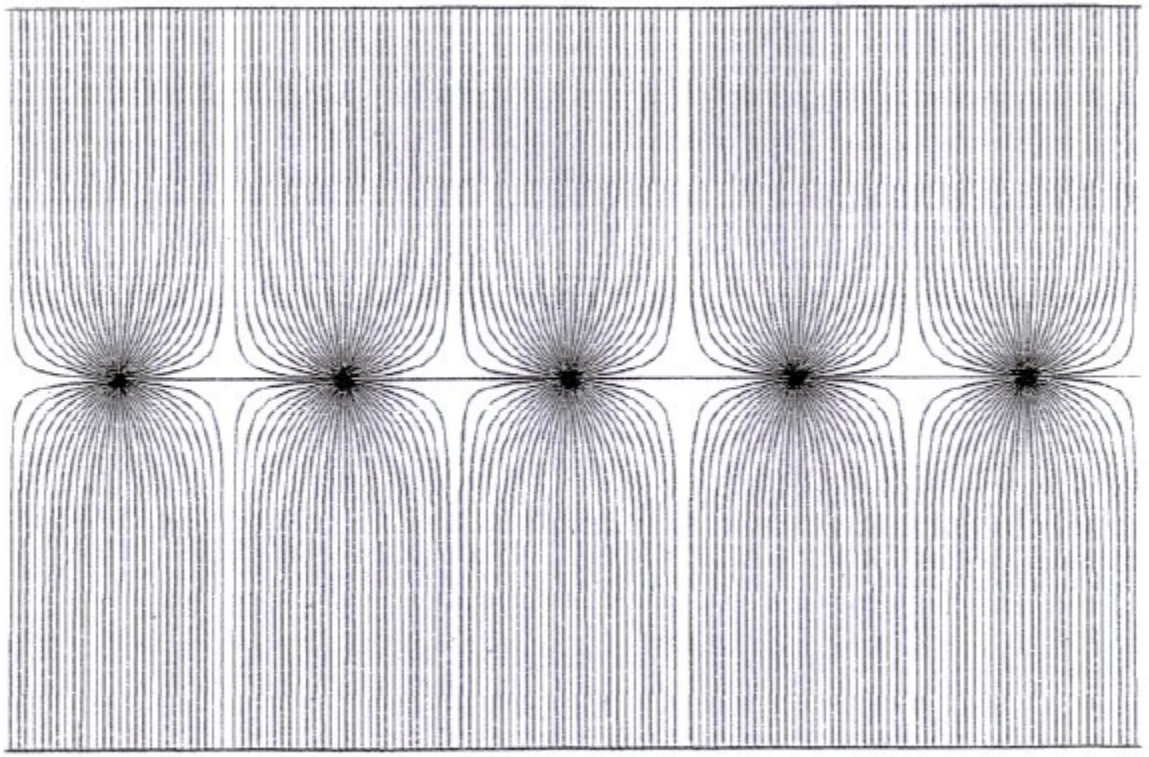

typical geometry of electric field lines in multi-wire proportional chamber

typical parameters:

$d = 2 - 4$ mm

$r_i = 15 - 25\ \mu$m

$L = 3 - 6$ mm

$U_0 =$ several kV

total area: many m^2

Fig. 4.3

Halbleiterdetektor

Streifendetektor

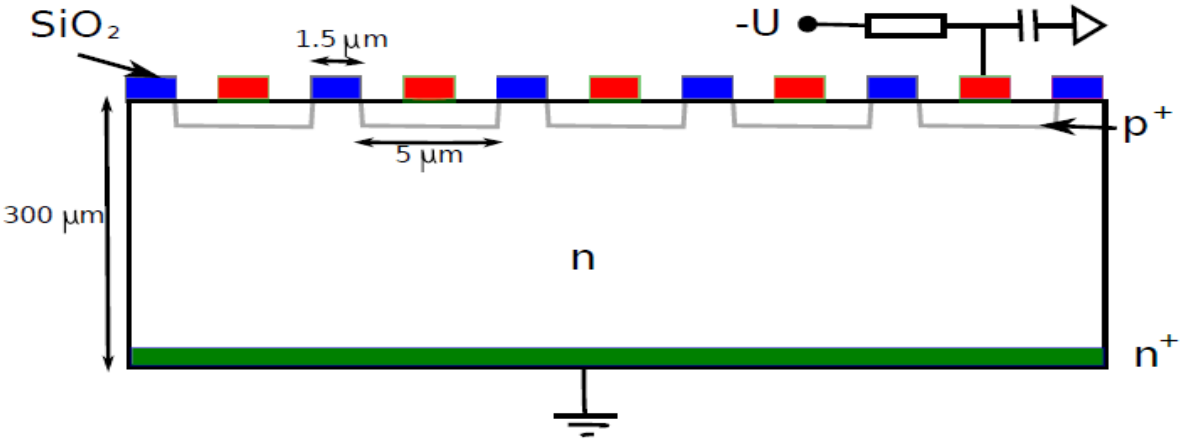

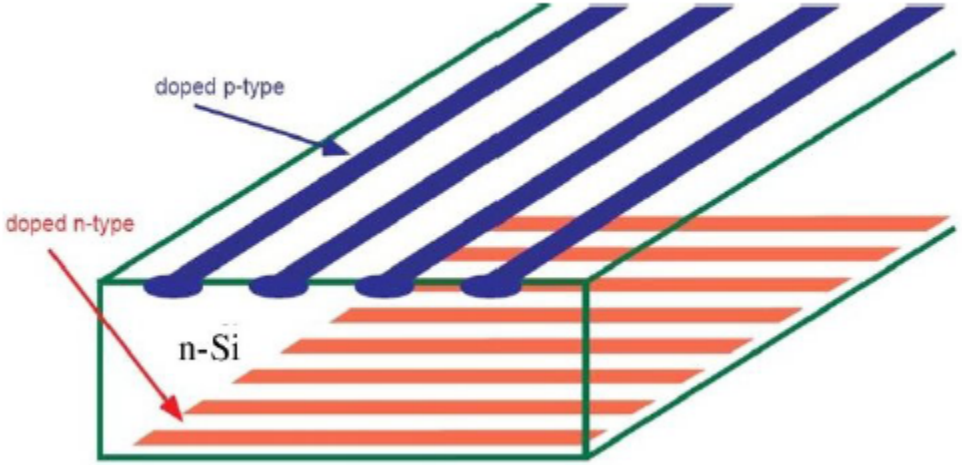

Pixeldetektor

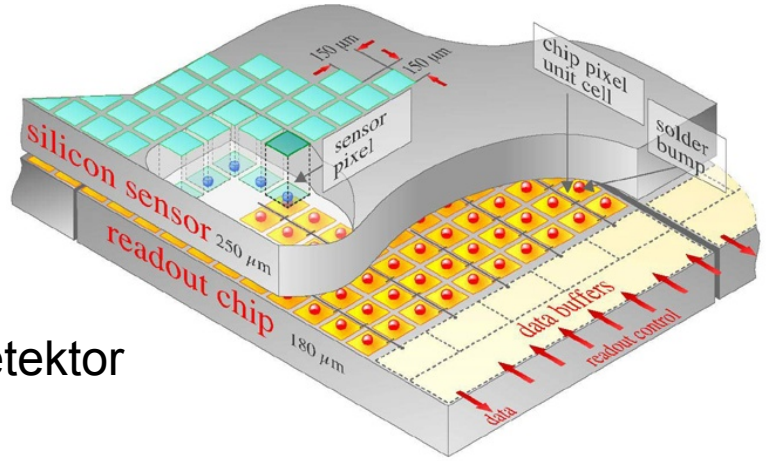

Fig. 4.4

ATLAS Pixel Detektor: 3 Lagen, 1.8 m^3, 80 Millionen Auslesekanäle

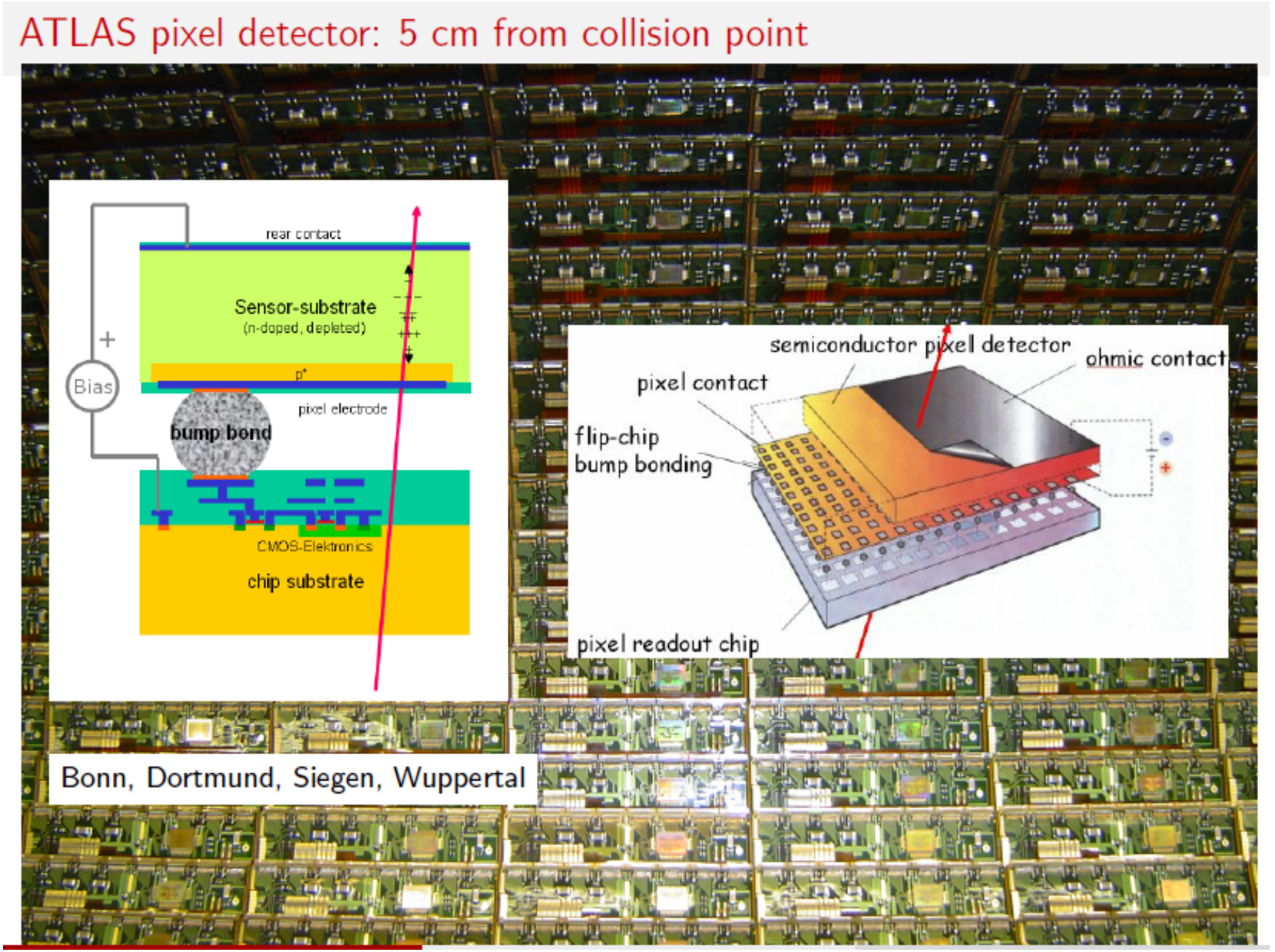

Fig. 4.5

szintilierende optische Fasern

to provide enough photoelectrons 4 layers
of fibres of 1 mm diameter
fibres in each column joined to same PMT
pixel of a multianode PMT
$\rightarrow$ 30 photoelectrons per muon

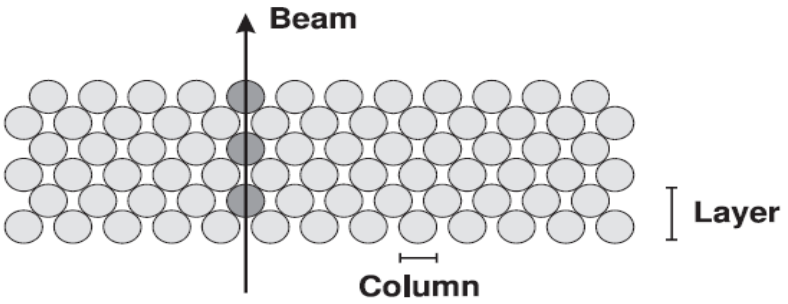

fibre configuration for scintillating fibre hodoscope with 3 layers of fibers

Fig. 4.6

Prinzip eines Sampling Kalorimeters

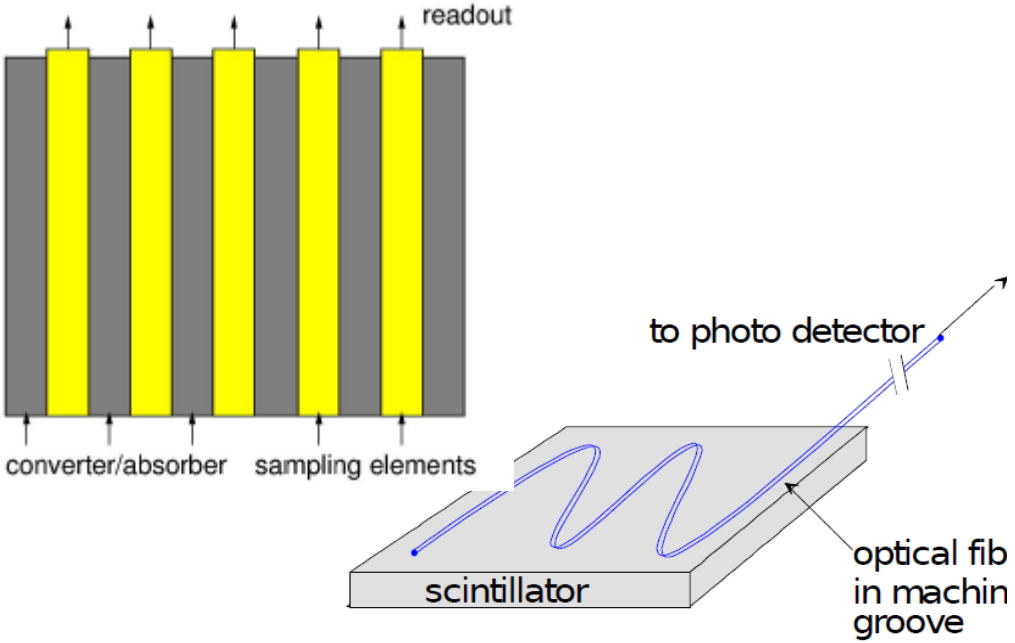

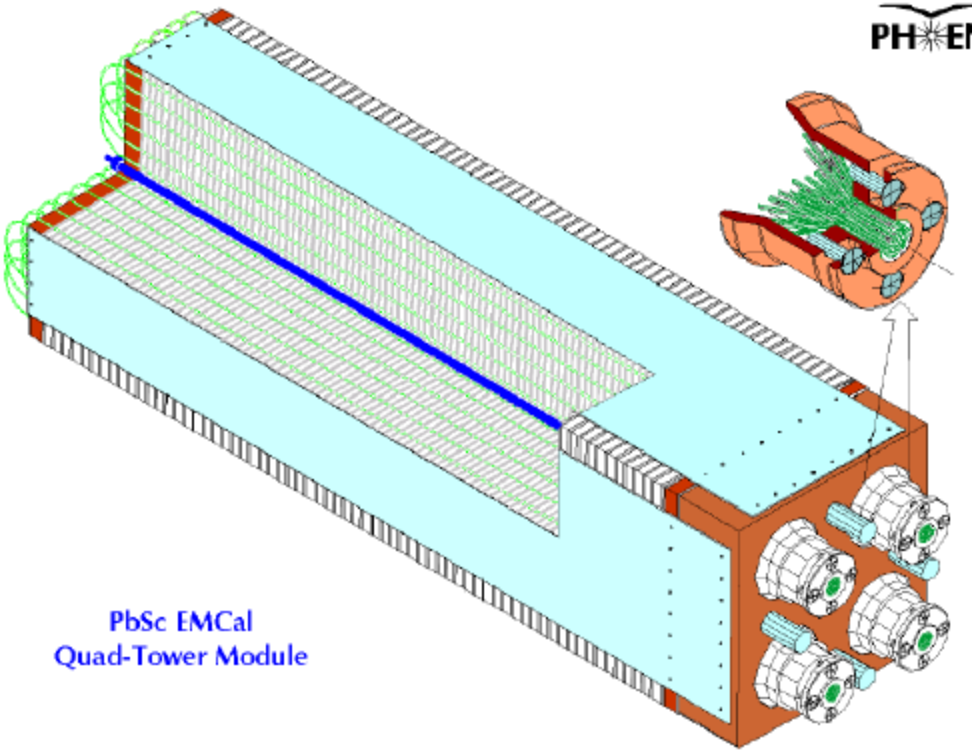

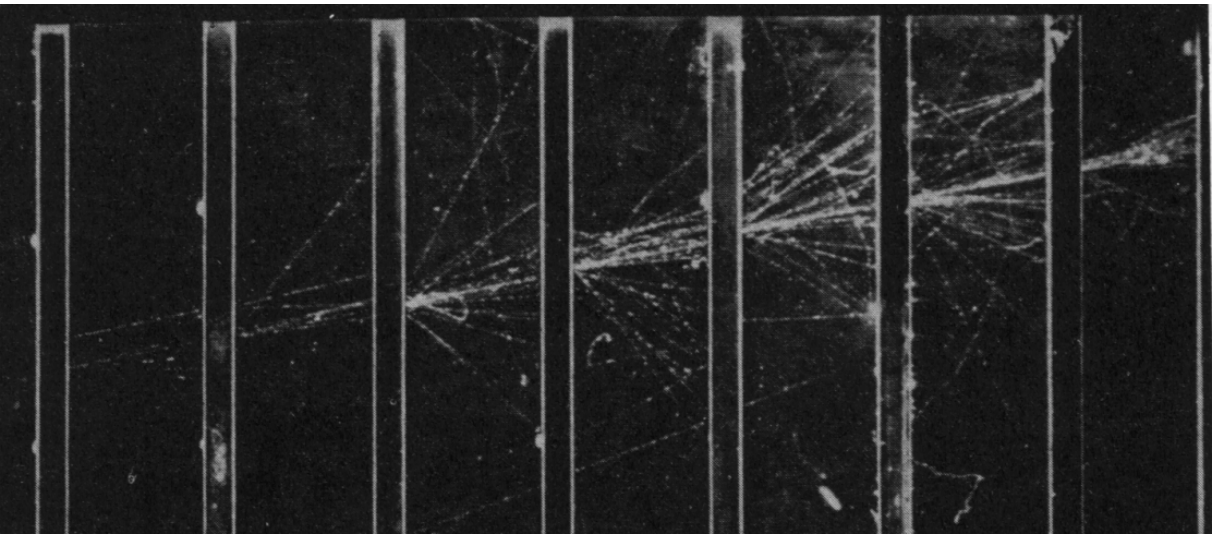

Photon-induced shower in a cloud chamber;
The intermediate black parts are lead blocks;
in addition, there is a magnetic field perpendicular to the figure plane

Fig. 4.7

Elektromagnetisches Kalorimeter aus Kristallen

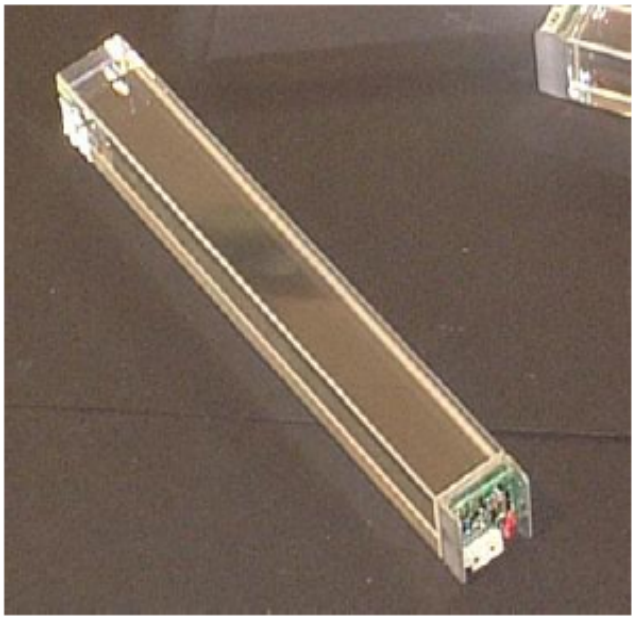

ALICE am LHC

array of $22 \times 22 \times 180$ cm^3 $PbWO_4$ crystals, depth 20 X_0
in total about 18 000 (same type as CMS)

characteristics: dense, fast, relatively radiation hard

emission spectrum $420 - 550$ nm
read out with 5×5 mm^2 avalanche photodiodes, $Q = 85\%$
charge-sensitive preamplifier directly mounted on APD

Fig. 4.8